Perturbed-angular-correlation measurements of trivalent indium defects in silver bromide

1996 J. Phys.: Condens. Matter 8 2679

(http://iopscience.iop.org/0953-8984/8/15/017)

J. Phys.: Condens. Matter **8** (1996) 2679–2694. Printed in the UK

Perturbed-angular-correlation measurements of trivalent indium defects in silver bromide

J C Austin, K Price, B K Patnaik and M L Swanson

Department of Physics and Astronomy, University of North Carolina, Chapel Hill, NC, 27599-3255, USA

Received 19 July 1995

Abstract. The structure and thermodynamics of defects involving In^{3+} ions and charge-compensating silver vacancies in AgBr were studied using perturbed angular correlation (PAC) spectroscopy. We saw two main defect configurations, both attributed to two Ag vacancies bound to the In^{3+} ion at next-nearest-silver-neighbour positions. A reversible transition occurred between the two configurations at approximately 80 K. The predominant complex below 80 K has $\nu_{Q1} = 40 \pm 1$ MHz and $\eta_1 \approx 0$. The 'zz' axis of the electric field gradient (EFG) tensor for this complex points along a $\langle 100 \rangle$ crystal axis. This complex is attributed to a collinear configuration with two silver vacancies at next-nearest-neighbour sites on opposite sides of the indium ion. The other complex, predominant between 80 K and the onset of diffusion-induced damping near 200 K, has $\nu_{Q2} = 20 \pm 1$ MHz and $\eta_2 = 0.35 \pm 0.15$. The 'zz' axis of the EFG tensor for this complex also lies along a $\langle 100 \rangle$ crystal axis. This complex is attributed to a configuration with two silver vacancies at next-nearest sites, forming a right triangle with the indium probe at the vertex. A third complex occurs near the transition, characterized by $\nu_{Q3} \approx 30$ MHz, but the quadrupole interaction parameters for this complex could not be precisely determined. The transition between the complexes that dominate above and below 80 K is reported and analysed in terms of equilibrium thermodynamics, allowing determination of differences in the formation enthalpy h and entropy s for the two complexes. We obtain $\Delta h = h_2 = h_1 = 40 \pm 15$ meV, and $\Delta s = s_2 - s_1 = (6 \pm 2)k_B$. Structural studies for other trivalent impurities in AgBr are briefly reviewed, and the PAC results are compared with those results and with earlier PAC results for In^{3+} in AgCl.

1. Introduction

A greater fundamental understanding of the properties of point defects in silver halides has resulted in a gradual improvement in the quality of practical photographic films [1]. An important innovation in recent years is the doping of silver halide grains in photographic emulsions with trivalent cation impurities to affect the relative concentration of photoelectrons and photoholes in order to influence film speed [2]. The photocarrier trapping behaviour of these defects is known to depend on the electronic configuration of the impurity and on the number and arrangement of trapped charge-compensating vacancies. A detailed understanding of this dependence remains elusive. A comprehensive useful theory of multivalent cation centres in silver halides will predict the lattice location of an impurity, the number and location of charge-compensating Ag vacancies, and a defect centre's photocarrier trapping behaviour. The present experimental study attempts to elucidate the first two areas.

Most of the work characterizing the atomic configurations of cation–vacancy complexes in silver halides has been done by electron paramagnetic resonance (EPR) and electron

0953-8984/96/152679+16$19.50

nuclear double resonance. Useful information has also been obtained via polarized Raman spectroscopy and perturbed angular correlation (PAC) spectroscopy.

EPR measurements in both AgCl and AgBr have shown that trivalent cations generally substitute for Ag ions and are usually completely charge compensated by two Ag vacancies. At sufficiently low temperatures these vacancies are trapped near the impurity at either nearest-neighbour (NN) positions (along ⟨110⟩ directions from the cation), or next-nearest-neighbour (NNN) positions (along ⟨100⟩ directions from the cation).

Yb^{3+}, Er^{3+} and Dy^{3+} ions have been studied in AgCl by EPR [3]. The major Yb spectrum indicates a complex of tetragonal symmetry, probably consisting of two NNN Ag vacancies on opposite sides of the Yb^{3+} ion. An orthorhombic site was also observed, consistent with a complex having two vacancies at NN sites, forming a right angle with the impurity ion at the vertex. A similar configuration was observed for Dy^{3+}. The Er signals are complicated and are not well understood.

Infrared spectroscopy indicates that the Rh^{3+} ion traps two Ag vacancies at NNN positions collinear with the Rh ion [4]. This complex is a deep electron trap (yielding the unpaired electron necessary for the EPR studies), and EPR measurements of the trapped state in AgBr (which presumably retains only one trapped vacancy) indicate a ⟨100⟩ axial symmetry below 100 K, consistent with a complex having a single vacancy at a NNN site. A temperature-reversible structural change occurs above 100 K, yielding at a higher temperature a 'compressed' configuration in which the trapped electron is delocalized. Above 220 K, the EPR spectrum degenerates into a single broad line, indicating a dynamic process such as motion of the trapped vacancy about the Rh^{2+} site [5]. More recent detailed measurements for Rh^{2+} in AgCl show a similar reversible behaviour. ENDOR measurements reveal that the low-temperature configuration is elongated along a ⟨100⟩ axis with a Ag vacancy and a NNN position in a plane perpendicular to the elongation axis. Above 110 K, the EPR hyperfine structure vanishes; this was explained by dynamic hopping of the elongation axis in a plane perpendicular to the Rh^{2+}-vacancy axis.

An EPR study of Ru^{3+} in both AgCl and AgBr indicates four different defect configurations [6]. One, observed for both AgCl and AgBr, has two NNN vacancies on opposite sides of the Ru ion (as for Rh and Yb). The other configurations in AgCl all have one NNN and one NN vacancy. These structures were not identified in AgBr, but equivalent structures are presumed to exist. Three similar defect complexes occur in Os^{3+}-doped AgCl and AgBr [7]. The predominant Os^{3+} centre in AgCl has two vacancies on opposite sides of the Os ion along a ⟨100⟩ axis. A second defect complex has NN and NNN vacancies oriented 135° apart in a {100} plane, and the least abundant defect has two NN vacancies oriented 180° apart, along ⟨110⟩. The results for AgBr appeared similar but were less well resolved.

An unusual case is the Fe impurity, which converts between divalent and trivalent charge states upon exposure to light or annealing in a halogen atmosphere. In certain conditions the trivalent Fe ion occupies a cube-centre interstitial site in both AgCl and AgBr, tetrahedrally coordinated with four Ag vacancies and four halogen ions [8]. Another interstitial configuration, similar to the tetrahedrally coordinated defect but having one of the NN Ag vacancies replaced with a Ag^{+} ion, was observed in AgCl by EPR [9]. This configuration was not observed in AgBr, but its existence was hypothesized.

Polarized Raman spectroscopy studies of Ir^{3+} ions in AgBr indicate that Ir occupies a site with tetragonal or lower symmetry. These results suggest a defect complex consisting of two NNN vacancies collinear with an Ir ion [10]. In contrast, similar experiments for Rh^{3+} in AgBr indicate a trigonal ⟨111⟩ symmetry (in apparent contradiction with earlier infrared spectroscopy measurements [4]), which, as Spoonhower [11] points out, cannot be explained

by a combination of a substitutional Rh ion and neighbouring vacancies. The possibility of $RhBr_3$ precipitates, which have ⟨111⟩ symmetry, was suggested; the Rh concentration was in the range 20–100 ppm in these experiments. The trigonal symmetry might, however, be attributable to a configuration such as that seen for the trivalent Fe ion in AgCl.

It is apparent from these results that trivalent cations generally occupy substitutional sites and—at low temperatures at least—trap two silver vacancies in various configurations. The configuration most commonly observed has two NNN vacancies situated on opposite sides of the ion along a ⟨100⟩ axis. However, other configurations (having, for example, both NN and NNN vacancies) sometimes occur in equilibrium, demonstrating that they are very close in energy.

Previously, we made detailed PAC measurements in AgCl using the radioactive isotope $^{111}In^{3+}$ as a cation probe. We found that two unique In–vacancy configurations predominate below 130 K, both having ⟨100⟩ axial symmetries [12]. Both of these defects apparently consist of two vacancies at NNN positions to the indium probe ion, one having vacancies collinear with respect to the In atom, the other having vacancies that form a right triangle with the probe ion at the vertex. Above 130 K, a transition to a completely different structure was observed [13]. We attributed this reversible transition to an entropy-driven change in the equilibrium structure of the defect centre. In some samples the higher-temperature defect converts to a defect having cubic symmetry, probably like the tetrahedral interstitial complex seen for Fe^{3+}. So it is tempting to assign this higher-temperature defect to a trigonal configuration such as that seen for Fe^{3+}, a logical precursor for the tetrahedral defect, but we were not able to make a definite assignment.

Near room temperature we observed the motion of trapped vacancies around the In atom, via diffusion-induced damping of the PAC signal at temperatures between 302 and 349 K. These results show that at least one of the two vacancies remains bound to the indium atom at least to 350 °C. We found that at room temperature the trapped vacancies hop around the impurity, between equivalent positions, at frequencies exceeding 10^8 Hz, indicating a dwell time of the order of 10 ns. Such rapid motion could be important in determining the behaviour of these centres as photocarrier traps. By measuring the orientation dependence of the damping parameters, we found a ⟨100⟩ axial symmetry for the resting configuration, indicating that between hops the vacancies dwell on NNN sites to the indium probe [14].

AgBr and AgCl are very similar materials in many respects, but significant subtle differences between the structures and behaviours of multivalent cation centres have been observed. The preceding discussion shows that different impurity ions may also behave quite differently in the same material. By determining and analysing the differences in terms of known properties of the different ions and materials, much can be learned about the factors that determine the defect structure and behaviour. In this paper we present PAC data for In^{3+}–vacancy defects in AgBr and relate these new results to our previous PAC data for AgCl, and to the results of investigations of other multivalent cations in the Ag halides.

2. Experimental procedure

The local environment of $^{111}In^{3+}$ ions in AgBr single crystals was studied by the $\gamma\gamma$ PAC method. High-purity AgBr crystals of approximate dimensions $2 \times 2 \times 12$ mm were oriented by Laue back-reflection x-ray scattering, polished and etched in sodium thiosulphate to remove surface contamination and mechanical strain. Polycrystalline samples were prepared by cutting a single crystal into about 100 pieces of approximately equal size before doping. Radioactive ^{111}In probe ions were introduced into the crystal by drying a $^{111}InCl_3$:HCl

solution in an HF-etched quartz capsule, placing the AgBr sample in the capsule and sealing it under Br gas. The sample was then annealed for 12–24 h at temperatures near 400 °C. The ^{111}In concentration was estimated to be 10^{14} cm^{-3} or 10^{-9} atomic fraction, from the activity of the ^{111}In (about 10 μ Ci or 10^{11} nuclei of ^{111}In) and from the depth of penetration, about 10 μm. PAC measurements were performed using a standard slow–fast coincidence apparatus, with four NaI detectors arranged at 90° intervals. All measurements reported in this paper were carried out in the dark, utilizing a closed-cycle He refrigeration unit.

In PAC, the local environment of probe ^{111}In nuclei are studied by measuring gradients of the electric field at the sites of the probe nuclei. The precession of the ^{111}In nuclei, caused by the interaction of the local electric field gradients (EFGs) with the nuclear electric quadrupole moment, results in a time dependence of the angular distribution of the anisotropic nuclear radiation pattern. The precession frequencies are measured via the time-dependent perturbation of the angular distribution between the gamma ray γ_1, which populates the intermediate ^{111}Cd state during the decay of ^{111}In, and the gamma ray γ_2, which depopulates that state. The measured precession occurs during this intermediate state, which has a lifetime of 84 ns and spin $I = \frac{5}{2}$. Experimentally, one NaI detector detects γ_1, starting a clock, and a second NaI detector detects γ_2, stopping the clock. PAC spectra $R(t)$ are obtained from the ratio of the coincidence counting rates between 90° and 180° detectors, as a function of the time between the detection of γ_1 and γ_2 [15]:

$$R(t) = A_{22}G^{eff}(t). \tag{1}$$

Here, A_{22} is a constant giving the maximum anisotropy of the distribution of γ_2 relative to γ_1 and, for static configurations,

$$G^{eff}(t) = f_0 + \sum_k f_k \left[s_{k0} + \sum_n s_{kn} \cos(\omega_{kn} t) \exp\left(-\frac{(\lambda_{kn} t)^2}{2} \right) \right] \tag{2}$$

is the time-dependent term arising from the quadrupole interaction. Here f_0 is the fraction of probe nuclei that are in unperturbed (cubic) sites, f_k is the fraction in a particular type of non-cubic site k, s_{kn} are coefficients that depend on the EFG symmetry and the orientation of the EFG tensor relative to the detectors, ω_{kn} are the nuclear precession frequencies that depend on the symmetry and magnitude of the EFG tensor for each site k, and λ_{kn} are damping coefficients that account for the finite widths in the EFG distributions, causing a spread in values of ω_{kn}.

The strength of the electric quadrupole interaction is often designated by $\nu_{Qk} = 10\omega_{k0}/3\pi$, where ω_{k0} is the fundamental precession frequency for a particular defect k. The interaction strength is given in terms of the EFG tensor by $\nu_{Qk} = (eQ/h)V_{zz}^k$, where Q is the quadrupole moment of the probe nucleus, V_{zz}^k is the largest principal-axis component of the EFG tensor and h is Planck's constant. The observed precession frequencies ω_{kn} depend on the asymmetry parameter η_k, defined by $\eta_k = |V_{xx}^k - V_{yy}^k|/V_{zz}^k$. The parameter η_k expresses the amount of deviation of the EFG tensor from axial symmetry. For axial symmetry, $\eta_k = 0$, $\omega_{k1} = \omega_{k0}$, and $\omega_{k1} : \omega_{k2} : \omega_{k3} = 1 : 2 : 3$.

It is well established that, under the sample preparation conditions that we use, indium occurs most often in the trivalent state in AgBr. EPR measurements provide no evidence for the paramagnetic In^{2+} centre, and PAC measurements do not indicate the magnetic interaction expected from a paramagnetic probe ion. In^+, if it exists, will occupy cubic–symmetric substitutional Ag sites at all temperatures. The fraction of indium atoms observed by PAC to occupy cubic-symmetric sites from 12 K to room temperature is at most about 10%. This, then, represents the upper limit on the amount of In^+. The remainder of the indium ions must be trivalent. Local charge neutrality requires that two Ag ion vacancies

be created for each trivalent ion. At sufficiently low temperatures these vacancies will be bound to the indium ion. During the nuclear decay of the ^{111}In probe, ^{111}Cd is created, and it is at this nucleus that the PAC measurements are made. Since the time scale of PAC measurements is of the order of 100 ns and since at low temperatures no ionic diffusion can occur in such a short time, it is actually a metastable Cd^{2+}–divacancy complex that is measured. Since ionic motion is frozen out during the 400 ns time window, the ionic configuration is roughly representative of In^{3+}. Phenomena that can occur on a time scale short compared with this time window, like electronic transitions and ionic relaxation, may be characteristic of this metastable Cd^{2+}–divacancy complex.

3. Results and discussion

A typical sequence of PAC measurements for AgBr:In is shown in figures 1 and 2, at temperatures between 12 and 100 K. Figure 1 shows $R(t)$ and figure 2 shows its Fourier transform for AgBr doped with concentrations of 1–10 ppb ^{111}In. A dramatic change occurs in the charge distribution around the In^{3+} ions at around 80 K. This transition between the low-temperature structure and the 100 K structure is generally (but not always) reversible, in the sense that, if the temperature is raised, the conversion seen in figures 1 and 2 occurs and, if the temperature is then lowered sufficiently slowly, the original configuration is restored. Fitting the experimental data of figures 1 and 2 to a theoretical equation such as (2) above yields detailed information about this transition. Below 80 K a single configuration predominates, characterized by $\nu_{Q1} = 40 \pm 1$ MHz, $\eta_1 = 0$. Above 80 K a different configuration predominates, characterized by $\nu_{Q2} = 20 \pm 1$ MHz and $\eta_2 = 0.35 \pm 0.15$. The large error reported for η_2 arises from a large sample-to-sample variation. The best value obtained for the polycrystalline specimen of figures 1 and 2 is $\eta_2 = 0.35$. The 102 K single-crystal spectra shown later in figure 5, probably the best and clearest data that we have, yield the larger value $\eta_2 = 0.45$. The transition between these two defects occurs via an intermediate structure characterized by $\nu_{Q3} \approx 30$ MHz. It is not possible to estimate η_3 with confidence (except to say that it is probably less than about 0.5) because of the overlap of the frequencies of f_3 with the other frequencies near the transition temperature.

We noted earlier that the reversibility between the low-temperature and 100 K structures is not complete. The degree of reversibility—the amount of the high-temperature configuration quenched in below the transition temperature—seems to depend on the cooling rate. The incomplete reversibility is apparent in figures 1 and 2, where the 20 MHz fraction (predominant above the transition) is significant in the 12 K measurement. This fraction is reduced at slightly higher measuring temperatures, where there is (apparently) sufficient thermal energy to allow the complex to relax into its preferred low-temperature state. The fraction of this defect increases again above the transition temperature.

The first task is to determine the nature of this transition. We may, first of all, rule out any mechanism involving long-range diffusion, since essentially all ionic diffusion is frozen out at 80 K (except, perhaps, for interstitial Ag ions, expected to occur only at a very low concentration). Accepted values of free-vacancy migration parameters (e.g. a migration enthalpy of 0.33 eV and a migration entropy of $1.7k_B$) predict one free vacancy jump every 10^8 s at 80 K. It is therefore clear that the change manifested in the data in figure 1 can only arise from a subtle local rearrangement.

The reversibility of the transition—incomplete though it may be—excludes the possibility that this is simply an annealing effect, in which a metastable configuration, given sufficient energy to overcome a barrier, relaxes into a new configuration of lower energy that is stable at any temperature. We are left with two possibilities: an electronic

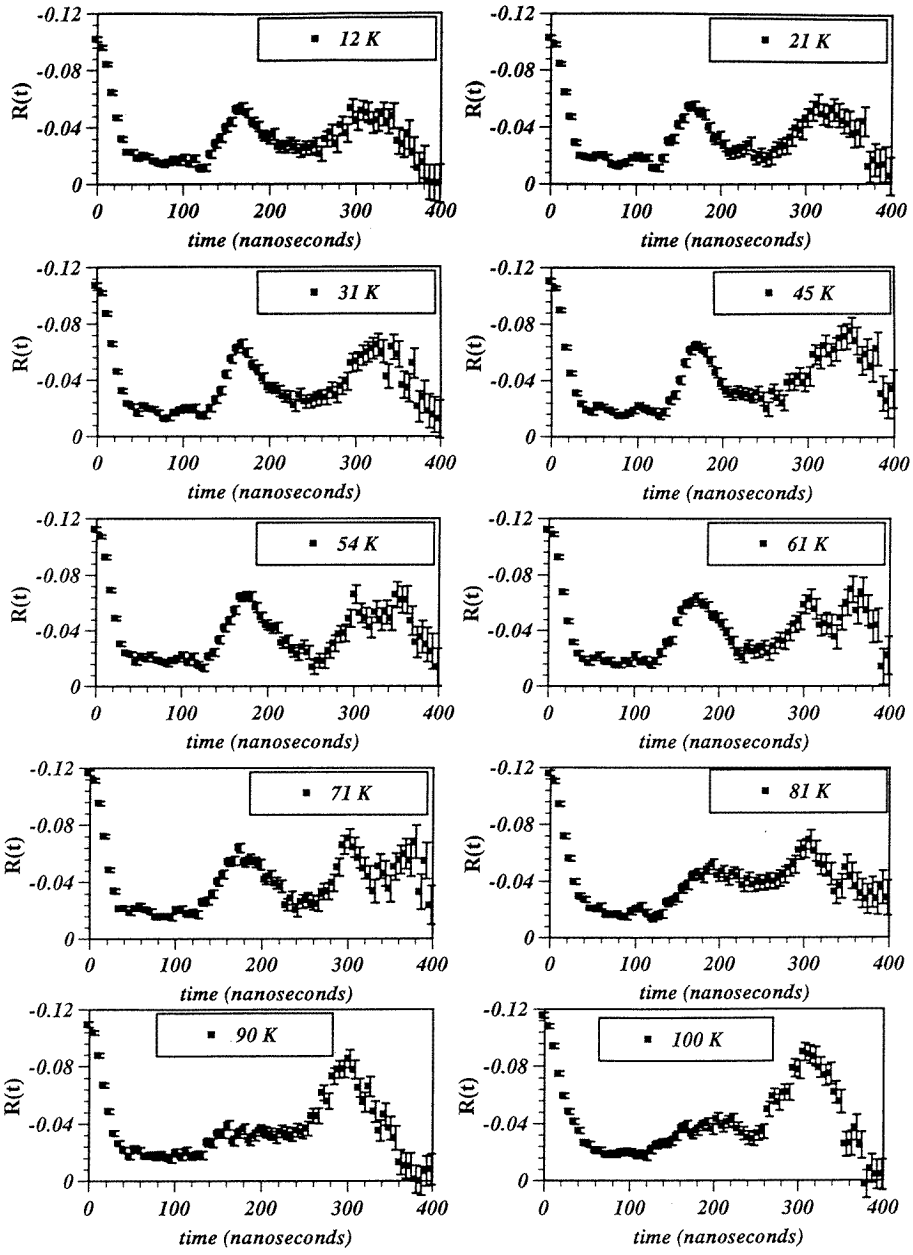

Figure 1. $R(t)$ for polycrystalline AgBr:In at several temperatures between 12 and 100 K.

transition, or an entropy-induced change in the equilibrium structure. It is unlikely that an electronic transition is involved. There are several reasons for this, but one is primary: the number of available traps far exceeds the number of electronic charge carriers, in the dark, at temperatures near 50 K. Also, indium is present at levels far below the levels of many other impurities that are likely to act as traps. So it is improbable that a significant fraction of the indium ions will trap carriers; such behaviour, if it occurs once, is unlikely to be

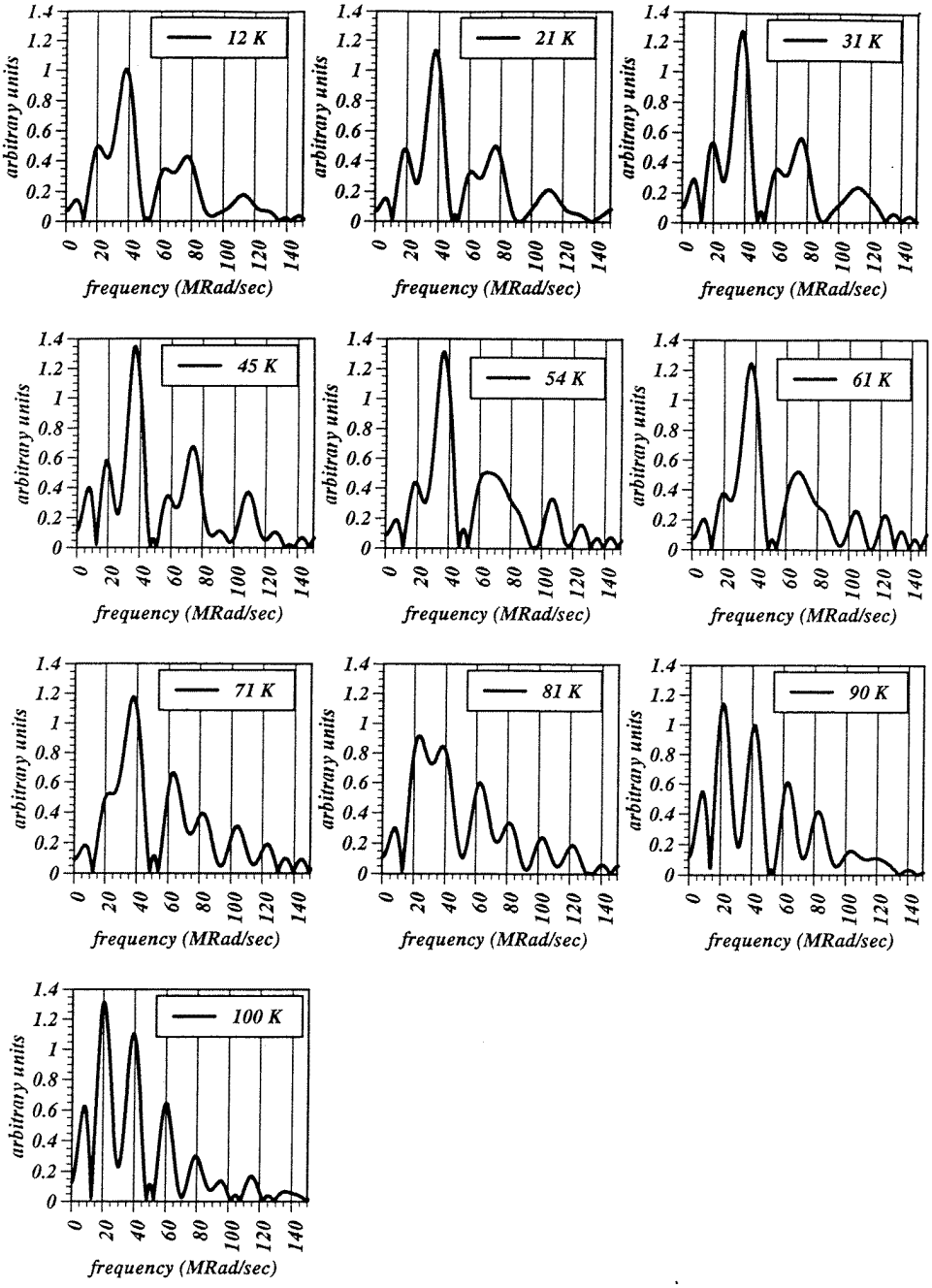

Figure 2. Fourier transform of $R(t)$ for AgBr:In at several temperatures between 12 and 100 K (from figure 1). Each unique defect structure results in three peaks in the Fourier transform. The angular frequency of the three peaks depends on ν_Q and the asymmetry parameter η. For $\eta = 0$, the angular frequency of the first peak is numerically equal to $\omega_1 = (3\pi/10)\nu_Q$, and the positions of the other peaks are determined by the relationship $\omega_1 : \omega_2 : \omega_3 = 1 : 2 : 3$. The ratio of the frequencies varies with η, subject to the condition $\omega_3 = \omega_1 + \omega_2$.

repeated and therefore be reversible with temperature.

The other alternative is the more reasonable; the availability of new vibrational modes at higher temperatures stabilizes a complex that is not preferred at lower temperatures. While a detailed analysis of such a phenomenon would be difficult (and certainly beyond the scope of this paper), it can be easily analysed using equilibrium thermodynamics. If the vibrational entropy term has a magnitude comparable to the enthalpy term in the Gibbs free energy, the stability curves for the two complexes can cross. We have made such an analysis previously for AgCl [13]. The ratio of the fractions of two different configurations, in an experiment carried out at constant pressure, is given by

$$\frac{f_2}{f_1} = \exp[s_2 - s_1/k_B]\ \exp[-(h_2 - h_1)/k_B T] \tag{3}$$

where s_1 and s_2 are the total entropies of formation, and h_1 and h_2 are the total enthalpies of formation, for the two configurations. Complex 1, which is lower in enthalpy but also has the smaller total entropy, is preferred below the transition temperature. Complex 2, which is higher in both enthalpy and entropy, is preferred above the transition temperature. By measuring the equilibrium fractions as a function of temperature and fitting them to equation (3), it is possible in principle to estimate the enthalpy difference Δh and the entropy difference Δs. Several factors complicate this analysis for the present case, particularly the freezing out of vacancy motion just below the transition temperature and the difficulty of precisely evaluating the fractions at temperatures near 80 K. A rough estimate is nevertheless possible; we obtain $\Delta h = h_2 - h_1 = 40 \pm 15$ meV, and $\Delta s = s_2 - s_1 = 6 \pm 2k_B$.

The incomplete reversibility indicates that the conversion occurs quite slowly—probably over minutes or hours at 80 K—which is not surprising considering the low temperature that it occurs at. It is notable that in one sample no reversibiilty at all was seen; when that sample was cooled slowly from 100 to 12 K, the configuration usually associated with the higher temperature dominated. Indeed, in this sample the 40 MHz defect was never seen. We believe that, given the very small energy differences between the different configurations, that the high-temperature configuration may be 'frozen in' by strain fields arising from other impurities and extended defects in close proximity to the indium–vacancy complexes, and thus that the stabilities may depend on subtle differences of sample preparation and measurement conditions.

We have made precise measurements of the dependence of the PAC spectra on the orientation of the detectors relative to the crystal axes. These measurements provide useful information on the structure of the different defects. These data and their analysis are presented in the following sections.

3.1. Structure of the 12 K defect complex

Below 80 K, the PAC spectrum is dominated by a single fraction, corresponding to a single defect complex, characterized by $\nu_{Q1} = 40 \pm 1$ MHz and $\eta_1 \approx 0$. Approximately half the indium probe atoms occupy such sites. The remainder occupy sites of cubic and near-cubic symmetry. These might be either uncompensated In^{3+} ions on substitutional sites, cubic-symmetric defects such as the tetrahedral complex seen for the Fe^{3+} ion, impurity clusters or extended defects. Figure 3 shows $R(t)$ and its Fourier transform for a single crystal of AgBr at 12 K, at two different detector orientations. Figure 3(a) shows $R(t)$ and its Fourier transforms for detectors aligned along $\langle 110 \rangle$ principal axes. Figure 3(b) shows $R(t)$ and its Fourier transform for precisely the same conditions except for the detector alignment, which in this case was along $\langle 100 \rangle$ crystal axes. These two spectra were measured consecutively,

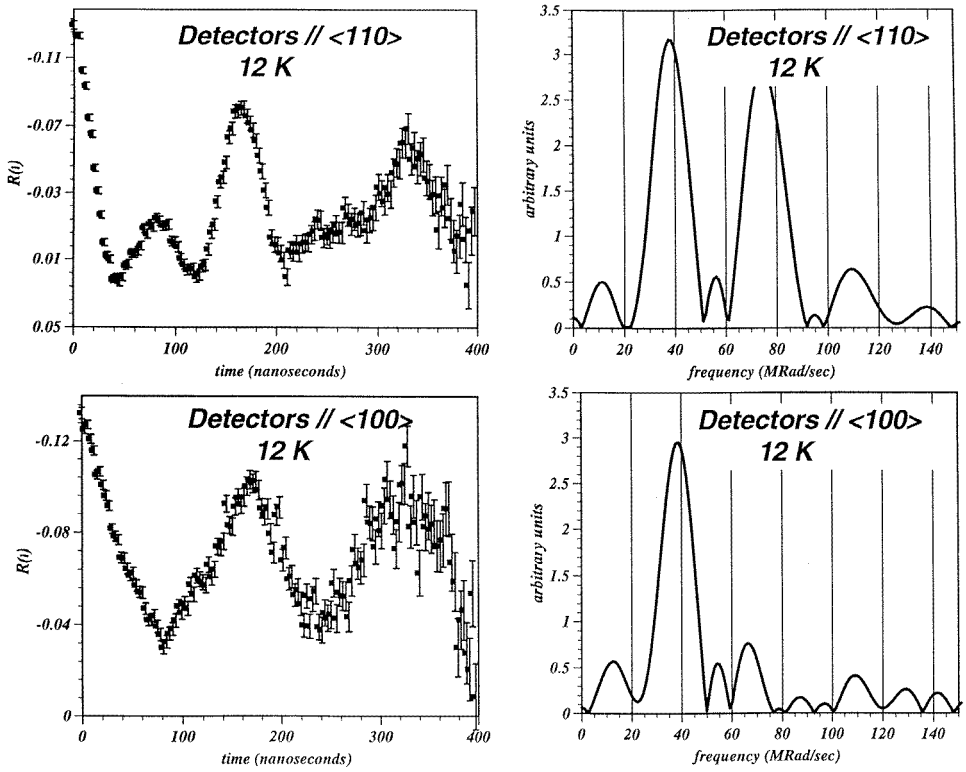

Figure 3. AgBr:In $R(t)$ and Fourier transform at 12 K for two different orientations of the NaI detectors relative to the crystal axes. The disappearance of the second peak in the Fourier transform when the detectors are aligned along ⟨100⟩ indicates a ⟨100⟩ orientation of the 'zz' axis of the defect complex's EFG tensor. See the caption to figure 2 for an explanation of the Fourier transform.

with no change in the measuring conditions except for the detector orientation. The ⟨110⟩ measurement was repeated following the ⟨100⟩ measurement, and the spectrum was found to be unchanged from the first ⟨110⟩ measurement (identical to within measurement error with figure 3(a)), verifying that the change seen from figure 3(a) to 3(b) is a result of the change in detector orientation. When the detectors were aligned along ⟨100⟩ crystal axes, the second peak of the Fourier transform—the peak at 75 Mrad s^{-1}—vanished completely. This is definitive evidence that the EFG tensor at the site of the indium probe nucleus has its 'zz' axis along ⟨100⟩ [14].

This defect is identical in every respect—except for the smaller quadrupole interaction frequency—with the 43 MHz defect seen in AgCl [12, 13]. The change in ν_Q between AgCl and AgBr is roughly what is expected from the change in the lattice constant. An analysis similar to that performed for this defect complex in AgCl leads to similar conclusions; we believe that this defect involves two vacancies bound at next-nearest silver sites to the indium, on either side of the indium ion. This complex, shown schematically in figure 4, has the most common configuration seen for trivalent impurities in silver halides, as discussed in the introduction. This complex is fully charge compensated, as expected at such low temperature, and it causes an EFG tensor with the observed ⟨100⟩ axial symmetry. Calculations of the magnitude of ν_Q are notoriously difficult to make precisely but our

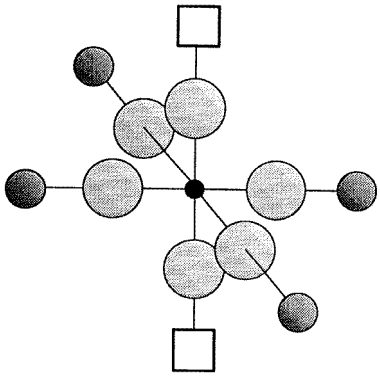

Figure 4. Proposed structure of the In–divacancy complex in AgBr below 80 K.

calculations based on a simple point-ion model are consistent with the measured value to within a factor of 2. This is good agreement considering the crudeness of the model, the extreme sensitivity of the electric quadrupole interaction to subtle differences in the local distribution of charge, and the importance in this calculation of the Sternheimer antishielding factor, whose value is only known for the free Cd ion. An inward relaxation of the nearest bromine neighbour of only 4% of the lattice constant will remove the discrepancy. Good agreement is obtained for those properties that depend primarily on the symmetry of the defect complex and less on the fine details of the analysis—such as η and the orientation fo the 'zz' axis.

3.2. Structure of the 100 K defect complex

Above 80 K and below the onset of diffusion-induced damping at around 200 K, the PAC spectra are dominated by a single well defined fraction, having a quadrupole coupling constant $\nu_{Q2} = 20 \pm 1$ MHz and an asymmetry parameter $\eta_2 = 0.35 \pm 0.15$. $R(t)$ spectra for AgBr measured at 102 K are shown in figure 5 for two different orientations of the detectors relative to the axes of our single-crystal specimen. The best estimate of the asymmetry parameter for this particular sample is at the high end of the range: $\eta_2 = 0.45 \pm 0.05$. As in the low-temperature spectra of figure 3, we see that, when the detectors are aligned along $\langle 100 \rangle$ crystal axes (figure 5(b)), the second peak—in this case the peak near 35 Mrad s^{-1}—vanishes. As before, this indicates a $\langle 100 \rangle$ alignment of the 'zz' axis of the EFG tensor. Note also the increase in the amplitude of the first peak when detectors are aligned along $\langle 100 \rangle$. This change, which occurs only for EFG tensors having η significantly different from zero, is also consistent with a $\langle 100 \rangle$ orientation of the EFG 'zz' axis. In principle it is possible to determine the orientation of the 'xx' and 'yy' axes of the EFG tensor from the dependence of the height of this first peak on the detector orientation, but the measured change in the amplitude of this peak was not consistent with any of the tabulated values. This probably indicates that the 'xx and 'yy' axes do not lie along any of the major crystallographic directions.

The value $\nu_{Q2} = 20$ MHz measured for this defect is quite close to the value $\nu_Q = 21.5$ MHz obtained for one complex seen in AgCl below its 130 K transition, and both of these defects have EFG $\langle 100 \rangle$ symmetries. The difference in frequency can be accounted for by the change in the lattice constant. Considering the similarities in the properties of

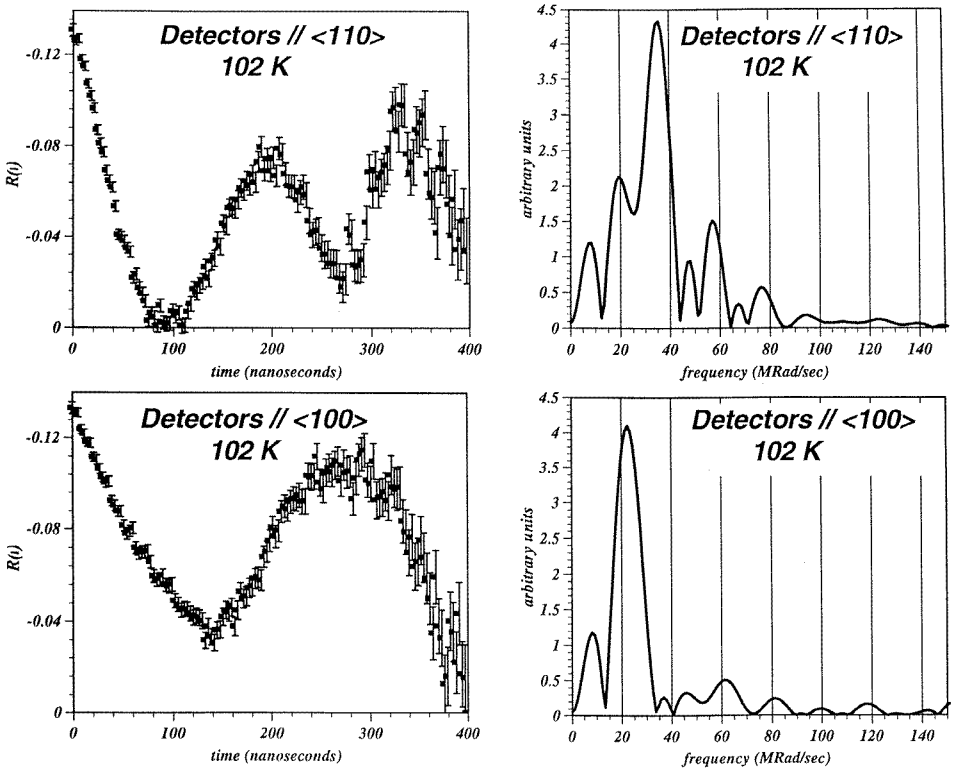

Figure 5. AgBr:In $R(t)$ and Fourier trnasform at 102 K for two different orientations of the NaI detectors relative to the crystal axes. The disappearance of the second peak in the Fourier transform when the detectors are aligned along ⟨100⟩ indicates a ⟨100⟩ orientation of the 'zz' axis of the defect complex's EFG tensor. See the caption to figure 2 for an explanation of the Fourier transform.

these two materials (AgCl and AgBr) it is reasonable to identify this 20 MHz complex in AgBr with the $\nu_Q = 21.5$ MHz, $\eta = 0$ complex in AgCl. In AgCl an indium–divacancy complex was proposed to account for this interaction, the two vacancies occupying next-nearest silver sites forming a right angle with the indium at the vertex [12, 13]. Such a complex is shown schematically in figure 6. According to a point-ion model such a structure would give the observed ⟨100⟩ EFG alignment, and a quadrupole coupling constant of exactly half the value for the collinear indium–divacancy complex (figure 4), consistent with the precise 2:1 ratio for the EFGs observed in both AgCl and AgBr.

The asymmetry parameter of the AgBr defect is dramatically different from the $\eta \approx 0$ reported for the AgCl defect [12]. If we are to assign the configuration of figure 6 to the 20 MHz complex in AgBr, this difference must be accounted for. The point-ion model applied to the analysis of the AgCl data adequately reproduced the observed asymmetry parameter and 'zz' axis even though the analysis did not consider relaxation or polarization. It seems probable that significant relaxation will occur, especially in the case of the right-angle complex shown in figure 6. Because of the missing silver ions, the net repulsion between the indium and the remaining Ag ions would probably cause the indium ion to relax in a ⟨110⟩ direction, as indicated by the arrow of figure 7. Some relaxation of the Br ions towards the indium probe ion would also be expected, but such relaxation cannot

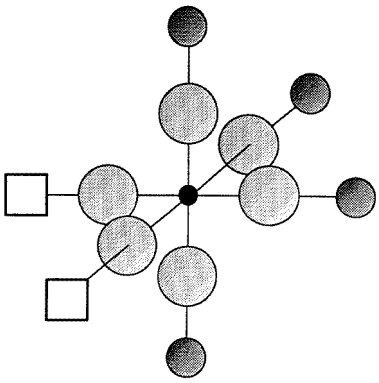

Figure 6. Proposed structure of the In–divacancy complex in AgBr between 80 K and the onset of diffusion-induced damping at 200 K.

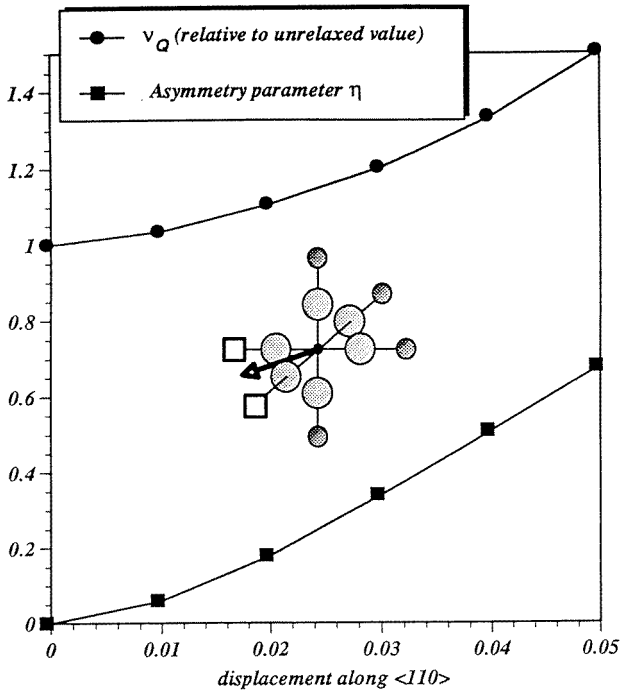

Figure 7. Quadrupole interaction frequency ν_Q and asymmetry parameter η as functions of the amount of relaxation of the In ion in the complex shown in the inset, in the direction shown by the arrow. The amount of relaxation is stated in terms of the fraction of the total diagonal distance across the unit cell $\sqrt{2}a$, where a is the lattice constant. The quadrupole interaction frequency ν_Q is given relative to the value calculated for zero relaxation.

change the asymmetry parameters. Figure 7 shows the dependence of ν_Q and η on the amount of relaxation of the indium probe ion, assuming a point-ion model and neglecting the relaxation of the other ions. Surprisingly, the orientation of the 'zz' axis is unaffected by this relaxation, as long as the relaxation is less than about 7% of the lattice constant.

The asymmetry parameter reaches the value $\eta = 0.35$ when the indium has relaxed by about 3% of the lattice constant. The larger value $\eta = 0.45$, obtained from the spectrum in figure 5, corresponds to a relaxation of nearly 4%. The reported value of $\eta = 0$ observed for AgCl indicates no relaxation at all, but considering the considerable experimental error a relaxation as large as 2% of the lattice constant is consistent with the AgCl data. Indeed, a re-examination of the AgCl data (figure 3 of [11]) reveals a reduction in the peak at 20 Mrad s^{-1} upon aligning the sample along $\langle 110 \rangle$; such a change is inconsistent with an asymmetry parameter less than 0.1.

As figure 7 shows, the 3–4% relaxation of the indium ion in the right-angle complex is inconsistent with the observed 2:1 ratio of ν_Q arising from the low- and high-temperature complexes (figures 4 and 6), if the 40 MHz complex is not also relaxed. However, if the indium ion in the collinear complex of figure 4 moves off-centre by a similar amount (about 4%) along the axis of the complex, the 2:1 ratio is restored, to a good approximation. Such relaxation does not change the value of the asymmetry parameter η.

To summarize, the structure of figure 6 is consistent with the 20 MHz defect in AgBr *and* the 21.5 MHz defect in AgCl *only* if the relaxation of the In ion is appreciably larger in the AgBr defect than in the AgCl defect. In order that the observed ratio $\nu_{Q1} : \nu_{Q2} = 2 : 1$ be maintained, it is necessary that the indium ion in complex 1 moves off-centre, along the symmetry axis of the complex, by approximately 4%. In both cases some relaxation of the Br ions will almost certainly occur, and this relaxation will affect the value of ν_Q, but it will not affect the asymmetry parameter η or—assuming that the Br ions relax by the same amount in both complexes—the ratio $\nu_{Q1} : \nu_{Q2} = 2 : 1$.

A comment is needed regarding the assignment of asymmetry parameter $\eta = 0$ to a complex that clearly lacks a fourfold or higher rotational symmetry axis. The asymmetry parameter describes the deviation of the EFG tensor, when expressed in its principal-axis system, from axial symmetry. The symmetry of the EFG tensor is in general different from the symmetry of the complex that causes the EFG tensor. Because the diagonal elements of the EFG tensor are invariant under spatial reflection, axial symmetry of the EFG tensor requires only what might be called a 'half-axial symmetry': $\rho(x) = \rho(y)$ and $\rho(-x) = \rho(-y)$. It is not necessary that $\rho(x) = \rho(-x)$ (here, ρ is the distribution of charge about the probe nucleus). Hence, the complex shown in figure 7 is 'axially symmetric' about the $\langle 100 \rangle$ direction perpendicular to the {100} plane containing the indium and vacancies.

In most AgBr samples there is little or no change in the PAC spectrum between 100 K and the onset of dynamic effects at about 200 K (presumably due to the hopping of vacancies around the indium probe ion). The onset of damping in AgCl occurred at a very similar but slightly higher temperature, around 210 K, suggesting that M^{2+}-bound-vacancy motion occurs somewhat more easily in AgBr than in AgCl at this temperature. This is just the opposite of what is expected for free vacancies (as estimated from values of entropy and enthalpy for AgCl and AgBr, which predict a slightly faster motion in AgCl than in AgBr [1]).

In certain samples a change occurs over several hours at temperatures near 200 K; a new, cubic-symmetric defect complex is formed, replacing complex 2. This transition apparently involves the trapping of a free vacancy and the formation of a tetrahedrally coordinated complex with an indium probe ion at an interstitial site, similar to the complex observed for the Fe^{3+} ion [8]. This complex is apparently stable only over a narrow range of temperatures, vanishing upon heating near 250 K and, in contrast to the similar defect seen in AgCl, upon cooling below about 150 K. The stabiity of such a negatively charged complex for the Fe^{3+} ion has been attributed to the electronic structure of the ferric ion, a structure that is not shared by the filled-shell In^{3+} ion; so a new explanation for the stability

of such complexes is required. A more detailed analysis of this transition and the resulting cubic-symmetric defect has been presented in a separate paper [16].

4. Conclusions

Several of our results deserve some additional comment. In both AgCl and AgBr, a reversible change occurs in the structure of the In–V_{Ag} complexes at fairly low temperatures. Similar reversible effects were observed at about 100 K by EPR for the Rh ion, but we believe that the electronic transition invoked to explain that transition is incompatible with the present experiment. We believe that the transition that we observed can be explained by equilibrium thermodynamics as a manifestation of lattice dynamics.

Both AgCl and AgBr PAC data indicate the existence of a defect in which the trivalent indium ion lies at the vertex of a right triangle with vacancies at NNN sites along ⟨100⟩. This defect was stable below the transition temperature (130 K) for AgCl, but above the transition temperature (80 K) for AgBr. No such complex has been reported by other techniques for any multivalent cation impurity in the silver halides. A simple analysis suggests that such a complex would occur with smaller probability than the collinear indium–divacancy complex, because of the repulsion between silver ions in the right-angle configuration. This difference is partially compensated by the larger configuration entropy of the right-angle complex; there are eight equivalent right-angle configurations and only three equivalent collinear configurations. Also polarization and relaxation effects are expected to offset the Coulomb repulsion, reducing the difference between the enthalpies of different configurations to below the values predicted by a naive model. Indeed, the preference of many ions for NNN vacancies, instead of NN vacancies, indicates that polarization is of comparable importance to the Coulomb repulsion in determining defect structure.

If our determination of the structure of the indium–divacancy complexes (figures 4 and 6) at the different temperatures in AgBr is correct, we may say, on the basis of our thermodynamic analysis, that the right-angle and collinear configurations differ in enthalpy by only about 40 meV. This analysis emphasizes another important factor in determining the equilibrium structure of these complexes: the vibrational entropy. It is well known that, for many phenomena (diffusion processes, for example), energy differences are often compensated by entropy differences. This phenomenological observation has been labelled as the Meyer–Neldel rule and has lately been rooted on firm theoretical ground [17]. It is also known that larger values of the vibrational entropy are often associated with less symmetric configurations [18]. These facts are consistent with our observations, where the larger formation enthalpy of less-symmetric configuration is largely offset by the larger vibrational entropy.

Although reversible structural transitions were seen in both AgCl and AgBr, the two transitions are quite different in detail. In AgCl no change was observed in the PAC spectrum below 100 K in any sample. It was assumed, consistent with known diffusion parameters, that significant ionic motion was frozen out below 100 K. At higher temperatures a reversible transition occurred, centred at about 130 K. The transition seen in AgBr occurred at a much lower temperature, about 80 K. The two configurations occurring in both materials (figures 4 and 6) both occurred below the transition temperature in AgCl, while in AgBr one appeared above the transition temperature and one appeared below. Above the transition temperature in AgCl the collinear configuration vanished completely and the right-angle fraction was much reduced. These were replaced by a new defect ($\nu_Q = 28.5$ MHz; $\eta \approx 0.2$) whose structure we were not able to determine, except to conclude that it does not have a ⟨100⟩ symmetry axis. It could possibly be attributed to the trigonal In_i^{3+}–$3V_{Ag}$, although there

are some problems with this interpretation. The PAC parameters for this defect bear some resemblance to the 30 MHz defect seen at intermediate temperatures in AgBr but, since the parameters for this defect could not be determined precisely, a detailed comparison is impossible.

Another notable difference between AgBr and AgCl is that the asymmetry parameter for the right-angle defect is larger in AgBr than in AgCl. In AgCl the EFG tensor for this defect was nearly axially symmetric. In AgBr this defect had an EFG tensor with an asymmetry parameter in the range $\eta = 0.2$–0.5. It is possible to account for this difference in η (a point-ion model) by assuming a 3–4% relaxation of the indium ion along the $\langle 110 \rangle$ direction bisecting the two indium–vacancy dipoles in the right-angle configuration, as shown in figure 7. Considering experimental error, the AgCl data can tolerate relaxation of only about 2%. This analysis implies that indium ions occurring in the right-angle configuration are less relaxed in AgCl than they are in AgBr. Perhaps this is a consequence of the larger size of the bromine ion, since this would allow more room on the lattice for the In^{3+} ion to relax. The larger polarizability of Br could also be significant. In order to preserve the 2:1 ratio obsreved for the two dominant defect complexes it is necessary that the indium ion in the collinear complex move off-centre, along the symmetry axis of the defect, by about 4%. The relaxation of the Br ions will of course also affect the value of ν_Q.

It is surprising that any change at all occurs in the structure of these defects at such low temperatures. The transition seen in AgBr is centred around 80 K, but a significant fraction of the indium-containing complexes is seen from figures 1 and 2 to rearrange even at 54 K. No significant ionic rearrangement has been observed before in AgBr at such a low temperature. According to the accepted diffusion parameters, diffusion of free vacancies and indium ions is frozen out at this temperature. It is possible that the extra energy injected into the lattice by the nuclear decay processes could excite some of the frozen defects over the diffusion barrier and into a new configuration. It is also possible that the diffusion of vacancies within these trivalent impurity–vacancy complexes is enhanced because there is so much open space in the lattice, due to the proximity of two vacancies and a small trivalent indium ion in place of the larger Ag^+.

Acknowledgments

The authors would like to thank Professor Larry Slifkin and Dr Myra Olm for helpful discussions. This work is supported by the National Science Foundation grant DMR-9200295.

References

[1] Friauf R J 1984 *The Physics of Latent Image Formation in Silver Halides* ed A Baldereschi, W Czaja, E Tosatti and M Tosi (Singapore: World Science) p 79
[2] Eachus R S and Olm M T 1989 *Cryst. Latt. Defects Amorph. Mater.* **18** 297
[3] Cook F B I and Smith M J A 1973 *J. Phys. C: Solid State Phys.* **6** 3785
[4] Kuan S 1974 *Inorg. Chem.* **13** 1256
[5] Eachus R S and Graves R E 1974 *J. Chem. Phys.* **61** 2860
[6] Corrigan D A, Eachus R S, Graves R E and Olm M T 1979 *J. Chem. Phys.* **70** 5676
[7] Eachus R S and Olm M T 1983 *Radiat. Eff.* **73** 69
[8] Hayes W, Pilbrow J and Slifkin L 1964 *J. Phys. Chem. Solids* **25** 1417
[9] Hay K A, Ingram D J E and Tomlinson A C 1968 *J. Phys. C: Solid State Phys.* **2** 1205
[10] Deri R J and Spoonhower J P 1984 *J. Chem. Phys.* **80** 5423

[11] Spoonhower J P 1982 *J. Phys. Chem. Solids* **43** 667
[12] Austin J C, Swanson M L, Hughes W C, Kao C T, Slifkin L M, Hofsäss H C and Frey E C 1990 *Phys. Rev.* B **42** 7699
[13] Austin J C, Swanson M L and Hughes Wm C 1993 *J. Phys.: Condens. Matter* **5** 8829
[14] Austin J C, Swanson M L and Hughes Wm C 1993 *Nucl. Instrum. Methods* **73** 429
[15] Wegner D 1987 *Hyperfine Interact.* **35** 803
[16] Austin J C and Swanson M L 1995 *J. Phys.: Condens. Matter* **7** 9747
[17] Yelon A and Movaghar B 1990 *Phys. Rev. Lett.* **65** 618
[18] Lannoo M and Bergoin J 1981 *Point Defects in Semiconductors I: Theoretical Aspects* (Berlin: Springer) p 23